Total multiphoton-ionization rates for an extremely short-ranged potential

W. Becker, J. K. McIver, and M. Confer
Center for Advanced Studies and Department of Physics and Astronomy, University of New Mexico, Albuquerque, New Mexico 87131
(Received 24 July 1989)

The total ionization rate by a plane-wave field in the long-wavelength approximation from a three-dimensional δ-function potential is reconsidered. Well into the above-threshold ionization regime, the Keldysh approximation turns out to yield virtually the exact ionization rate for circular polarization. For multiphoton orders in excess of $n \sim 10$, lowest-order perturbation theory only holds for intensities much lower than those employed in current experiments. For moderate intensities, the total ionization rate is very well approximated by a slope of $N+k$ with integer $k \geq 1$. Within the range of most experimental interest where one or several channels are suppressed by the ponderomotive barrier, the slope is again near N and decreasing with increasing intensity.

I. INTRODUCTION

One of the most interesting aspects of above-threshold ionization (ATI) is the very different behavior of the total ionization rate and the partial ionization rates (where the electron absorbs a definite number of photons) as a function of the intensity I of the ionizing field. The partial rates exhibit a pronounced and definitely nonperturbative dependence on the intensity. This is evident from those features such as peak switching and peak suppression, which first raised the interest in ATI phenomena. On the other hand, for the same intensities, the total ionization rate still follows more or less closely the I^N dependence (with N close to the minimum number of photons that is required for ionization) that had been characteristic of all multiphoton ionization rates before the first observation of ATI.[1] The persistence of the approximate I^N behavior of the total rate which is predicted by lowest-order perturbation theory (LOPT) has thus far not been seriously challenged by either experiment or theory. Experimentally, I^N behavior has been observed well into the intensity region where many electron energy channels are already closed due to the ponderomotive potential barrier.[2] All deviations from the I^N shape thus far have been attributed to saturation. Only very recently are there indications of a slope smaller than N below saturation.[3] However, it seems that the situation must still be considered inconclusive. On the theoretical side, many numerical simulations demonstrate the persistence of the I^N behavior of the total rate up to fields where the partial rates are no longer described by anything near perturbation theory.[4,5] Analytical results are not available.

In this paper, we intend to shed some light on this situation by investigating an (almost) analytically solvable model of multiphoton ionization: a three-dimensional δ-function potential including a regularizing operator. This model potential, which is originally due to Fermi,[6] has been considered in the context of applications in nuclear physics,[7] many-body physics,[8] and atomic physics.[9–11] Due to the presence of the regularizing operator it has exactly one bound state (without it would have none) like its one-dimensional counterpart. Hence it would be expected to give a reasonable description of the H^- ion, which has just one bound state. How far results derived from this potential can be applied to ATI of rare gas atoms is, of course, debatable. It might serve as a realistic approximation of a short-range potential.[12] While it clearly does not apply whenever any resonant state is involved it might at least point in the right direction in the case of nonresonant multiphoton ionization. Moreover, if the model should turn out to be in conflict with experimental data, these differences could be attributed to the long-range character of the actual binding potential.

The paper is organized as follows. In Sec. II A we rederive the Keldysh approximation. Following Keldysh[13] we use the electric field gauge throughout, which leads immediately to gauge-invariant results even if the external field is not properly turned on and off. In Sec. II B we specialize our results to the three-dimensional δ-function well. In this case, the electric field gauge has an additional advantage over the $\mathbf{p}\cdot\mathbf{A}$ gauge: in the latter, due to the momentum dependence of the regularized δ-function potential, minimal substitution generates an additional electron-field coupling term (which was omitted in Ref. 9. It has been shown[10] that it makes no contribution to the ionization *rates,* but it might affect the wave function). No such term exists in the electric field gauge. Various forms for the total ionization rate are obtained. In Sec. II C we compare for the δ-function potential the Keldysh approximation with Berson's solution,[9] which is exact in the context of the quasienergy formalism. It turns out that the Keldysh approximation is exact up to the neglect of the Stark shift of the ground state. Section III discusses the total ionization rate as a function of the applied field for various multiphoton orders, based on numerical evaluation of a double series. A possibly unexpected result is that for high multiphoton orders the total rate already deviates from the I^N behavior predicted by

lowest-order perturbation theory (with N the minimum number of photons required for ionization in a weak field) for intensities far below those where channels close due to the ponderomotive barrier. Finally, Sec. IV summarizes our conclusions. Throughout this paper, we use units such that $\hbar=c=1$.

II. AN ATOM IN A PLANE-WAVE FIELD

A. Derivation of the Keldysh approximation

We want to consider an atom that is subjected to a finite pulse of an electromagnetic wave. In fact, we only consider one electron bound by a static potential. Prior to the arrival of the pulse the electron is in the ground state with the wave function $\psi_0^{(0)}(\mathbf{r},t)=\psi_0^{(0)}(\mathbf{r})\exp(i|E_0|t)$ with $|E_0|$ the binding energy. The probability that the electron is ionized into a final state with momentum $\mathbf{p}$ and wave function $\psi_{\mathbf{p}}^{(0)}(\mathbf{r},t)$ is determined by the square of the matrix element

$$M_{\mathbf{p}}=\lim_{t\to\infty}\int d^3r\,\psi_{\mathbf{p}}^{(0)}(\mathbf{r},t)^*\psi_0(\mathbf{r},t)\ , \tag{2.1}$$

where $\psi_0(\mathbf{r},t)$ is given by the time evolution of the initial state $\psi_0^{(0)}(\mathbf{r},t)$, viz.,

$$\psi_0(\mathbf{r},t)=\lim_{t'\to-\infty}\int d^3r'\,iG_+(\mathbf{r}t,\mathbf{r}'t')\psi_0^{(0)}(\mathbf{r}',t')\ . \tag{2.2}$$

Here $G_+(\mathbf{r}t,\mathbf{r}'t')$ denotes the retarded propagator in the presence of both the ionizing field $\mathbf{E}(t)$ described in the dipole approximation and the binding potential $V(\mathbf{r})$

$$\left[i\frac{\partial}{\partial t}-\frac{\mathbf{p}^2}{2m}+e\mathbf{r}\cdot\mathbf{E}(t)-V(\mathbf{r})\right]G_+(\mathbf{r}t,\mathbf{r}'t')=\delta(t-t')\delta(\mathbf{r}-\mathbf{r}')\ . \tag{2.3}$$

The unperturbed propagator $G_+^{(0)}(\mathbf{r}t,\mathbf{r}'t')$ satisfies the same equation with the term $e\mathbf{r}\cdot\mathbf{E}(t)$ missing. The full propagator then obeys the integral equation

$$G_+=G_+^{(0)}+G_+^{(0)}H_IG_+=G_+^{(0)}+G_+H_IG_+^{(0)}\ , \tag{2.4}$$

written in shorthand operator notation with $H_I\to-e\mathbf{r}\cdot\mathbf{E}(t)$. Using Eq. (2.2) and the second version of Eq. (2.4) in Eq. (2.1) we obtain, exploiting the orthogonality of the eigenfunctions of $H_0=\mathbf{p}^2/2m+V(\mathbf{r})$,

$$M_{\mathbf{p}}=\lim_{t\to\infty}\int d^3r\,d^3r'\,dt'\,\psi_{\mathbf{p}}^{(0)}(\mathbf{r},t)^*G_+(\mathbf{r}t,\mathbf{r}'t')\times[-e\mathbf{r}'\cdot\mathbf{E}(t')]\psi_0^{(0)}(\mathbf{r}',t')\ , \tag{2.5}$$

which is still exact. Both wave functions are in the presence of the binding potential, but in the absence of the field.

The Keldysh approximation replaces $\psi_{\mathbf{p}}^{(0)}(\mathbf{r}t)$ by a plane wave with momentum $\mathbf{p}$ and energy $E_{\mathbf{p}}=\mathbf{p}^2/2m$, and the full propagator G_+ by the propagator $G_+^{(E)}$ in the presence of merely the field [i.e., with the potential $V(\mathbf{r})$ missing in Eq. (2.3)]. The corresponding approximation in the $\mathbf{p}\cdot\mathbf{A}$ gauge, which is not gauge invariant, is referred to as the Keldysh-Faisal-Reiss (KFR) approximation.[5,13–15] We notice that

$$\lim_{t\to\infty}\int d^3r(2\pi)^{-3/2}e^{i(E_pt-\mathbf{p}\cdot\mathbf{r})}iG_+^{(E)}(\mathbf{r}t,\mathbf{r}'t')=\psi_{\mathbf{p}}^{(E)}(\mathbf{r}',t')^*\ ,$$

where

$$\psi_{\mathbf{p}}^{(E)}(\mathbf{r},t)=(2\pi)^{-3/2}\times\exp\left[i\left[\pi(t)\cdot\mathbf{r}-\frac{1}{2m}\int^t d\tau\,\pi^2(\tau)\right]\right] \tag{2.6}$$

is the Volkov wave function in the electric field gauge and $[\mathbf{E}(t)=-\partial\mathbf{A}(t)/\partial t]$

$$\pi(t)=\mathbf{p}-e\,\mathbf{A}(t)\ . \tag{2.7}$$

The lower limit of the integral in Eq. (2.6) only contributes an irrelevant phase and can be left arbitrary. Thus the Keldysh approximation yields the matrix element

$$M_{\mathbf{p}}^{(K)}=-i\int d^3r\,dt\,\psi_{\mathbf{p}}^{(E)}(\mathbf{r},t)^*[-e\mathbf{r}\cdot\mathbf{E}(t)]\psi_0^{(0)}(\mathbf{r},t)\ . \tag{2.8}$$

The matrix element (2.8) can be rewritten in a different form whose evaluation is much simpler in most cases. Noticing that

$$-e\mathbf{r}\cdot\mathbf{E}(t)\exp[-i\pi(t)\cdot\mathbf{r}]=-i\frac{\partial}{\partial t}\exp[-i\pi(t)\cdot\mathbf{r}]\ , \tag{2.9}$$

we integrate by parts on the right-hand side (rhs) of Eq. (2.8) and obtain

$$M_{\mathbf{p}}^{(K)}=-i\int d^3r\,dt\,\psi_{\mathbf{p}}^{(E)}(\mathbf{r},t)^*\times\left[-\frac{1}{2m}\pi^2(t)+i\frac{\partial}{\partial t}\right]\psi_0^{(0)}(\mathbf{r},t)\ .$$

The boundary terms at $t\to\pm\infty$ vanish for a field pulse of finite duration [since no harmonics of the field frequency are there to cancel the rapidly oscillating term $\exp(i|E_0|t)$]. With the help of

$$\frac{\pi^2(t)}{2m}\exp[-i\pi(t)\cdot\mathbf{r}]=-\frac{1}{2m}\nabla^2\exp[-i\pi(t)\cdot\mathbf{r}]\ ,$$

a further integration by parts yields

$$M_{\mathbf{p}}^{(K)}=-i\int d^3r\,dt\,\psi_{\mathbf{p}}^{(E)}(\mathbf{r},t)^*\times\left[-\frac{1}{2m}\nabla^2+i\frac{\partial}{\partial t}\right]\psi_0^{(0)}(\mathbf{r},t)=-i\int d^3r\,dt\,\psi_{\mathbf{p}}^{(E)}(\mathbf{r},t)^*V(\mathbf{r})\psi_0^{(0)}(\mathbf{r},t)\ . \tag{2.10}$$

In this case it is obvious that the boundary terms vanish. The matrix element $M_{\mathbf{p}}^{(K)}$ in the form of Eq. (2.8) or (2.10) is manifestly gauge invariant: in view of Eqs. (2.6) and (2.7) it only depends on the electric field strength $\mathbf{E}(t)$ and the mechanical momentum $\pi(t)$.

The total transition rate per time is obtained by summing $|M_{\mathbf{p}}^{(K)}|^2$ over all momenta

$$\Gamma=\lim_{T\to\infty}\frac{1}{T}\int d^3p\,|M_{\mathbf{p}}^{(K)}|^2$$
$$=\lim_{T\to\infty}\frac{1}{T}\int d^3r\,dt\,d^3r'dt'iG^{(E)}(\mathbf{r}t,\mathbf{r}'t')$$
$$\times V(\mathbf{r})\psi_0^{(0)}(\mathbf{r},t)^*V(\mathbf{r}')\psi_0^{(0)}(\mathbf{r}',t')\ . \quad (2.11)$$

Here $G^{(E)}$ denotes the homogeneous Green's function of the electron in the presence of the field

$$G^{(E)}(\mathbf{r}t,\mathbf{r}'t')=-i\int d^3p\ \psi_{\mathbf{p}}^{(E)}(\mathbf{r},t)\psi_{\mathbf{p}}^{(E)}(\mathbf{r}',t')^*$$
$$=e^{i\mathcal{R}(\mathbf{r}t,\mathbf{r}'t')}e^{-i\mathcal{M}(t,t')}G^{(0)}(\mathbf{r}t,\mathbf{r}'t')\ , \quad (2.12)$$

where

$$\mathcal{R}(\mathbf{r}t,\mathbf{r}'t')=-e\left[\mathbf{A}(t)\cdot\mathbf{r}-\mathbf{A}(t')\cdot\mathbf{r}'-\frac{\mathbf{r}-\mathbf{r}'}{t-t'}\int_{t'}^{t}d\tau\ \mathbf{A}(\tau)\right], \quad (2.13)$$

$$\mathcal{M}(t,t')=\frac{e^2}{2m}\left[\int_{t'}^{t}d\tau\ \mathbf{A}^2(\tau)-\frac{1}{t-t'}\left[\int_{t'}^{t}d\tau\ \mathbf{A}(\tau)\right]^2\right], \quad (2.14)$$

and

$$G^{(0)}(\mathbf{r}t,\mathbf{r}'t')=\left[\frac{im}{2\pi(t-t'-i\epsilon)}\right]^{3/2}\times\exp\left[i\frac{m(\mathbf{r}-\mathbf{r}')^2}{2(t-t')}\right] \quad (2.15)$$

is the homogeneous Green's function of the free electron.

B. Application to a δ-function well

For the attractive three-dimensional δ-function potential

$$V(\mathbf{r})=\frac{2\pi}{m\kappa}\delta(\mathbf{r})\frac{\partial}{\partial r}r\ , \quad (2.16)$$

the wave function of the ground state is

$$\psi_0^{(0)}(\mathbf{r},t)=\left[\frac{\kappa}{2\pi}\right]^{1/2}\frac{e^{-\kappa r}}{r}e^{i|E_0|t}\ , \quad (2.17)$$

with $|E_0|=\kappa^2/2m$. For a circularly polarized field

$$\mathbf{A}(t)=a(\hat{\mathbf{x}}\cos\omega t+\hat{\mathbf{y}}\sin\omega t)\ , \quad (2.18)$$

the evaluation of the Keldysh matrix element $M_{\mathbf{p}}^{(K)}$ in the form (2.10) is straightforward. The result is

$$M_{\mathbf{p}}^{(K)}=i\frac{\sqrt{\kappa}}{m}\sum_n e^{in\delta}J_n\left[\frac{eap_T}{m\omega}\right]\times\delta\left[|E_0|+\frac{1}{2m}[\mathbf{p}^2+(ea)^2]-n\omega\right], \quad (2.19)$$

with p_T the absolute value of the momentum transverse to the propagation direction of the field and

$$\tan\delta=\frac{p_y}{p_x}\ .$$

The evaluation starting from the form (2.8) is less straightforward. Since we are here using a field of infinite extent it is not quite obvious that the integration by parts, which established the equality of the expressions (2.8) and (2.10), is still legitimate. We defer a discussion of this point to the Appendix, noting here only that an explicit evaluation of Eq. (2.8) does reproduce the result (2.19).

Squaring Eq. (2.19) and integrating over the absolute value of the electron's momentum gives the transition rate per time and solid angle

$$d\Gamma=\frac{1}{T}\left[\int p^2dp\,|M_p^{(K)}|^2\right]d\Omega=\sum_n d\Gamma_n\ ,$$
$$d\Gamma_n=\frac{\kappa}{2\pi m}p_nJ_n^2\left[\frac{eap_n\sin\theta}{m\omega}\right]d\Omega\ , \quad (2.20)$$

with

$$p_n=[2m(n\omega-|E_0|)-(ea)^2]^{1/2}\ . \quad (2.21)$$

Summing $d\Gamma_n$ over all channels and integrating gives one of several equivalent expressions for the total ionization rate. Alternatively, starting from Eq. (2.11), we obtain

$$\Gamma=\lim_{T\to\infty}\frac{i}{T}\frac{2\pi\kappa}{m^2}\int_{-T/2}^{T/2}dt\,dt'G^{(E)}(0t,0t')e^{-i|E_0|(t-t')}\ . \quad (2.22)$$

The evaluation is comparatively simple since $\mathcal{R}(0t,0t')\equiv0$ and for the circularly polarized field (2.18)

$$\mathcal{M}(t,t')=\frac{(ea)^2}{2m}(t-t')\left[1-\left[\frac{\sin[\omega(t-t')/2]}{\omega(t-t')/2}\right]^2\right] \quad (2.23)$$

depends only on the time difference. Therefore

$$\Gamma=\frac{2\pi\kappa}{m^2}\left[\frac{m}{2\pi i}\right]^{3/2}\int_{-\infty}^{\infty}\frac{d\tau}{(\tau-i\epsilon)^{3/2}}\exp(-i|E_0|\tau)\exp\left\{-i\frac{(ea)^2}{2m}\tau\left[1-\left[\frac{\sin(\omega\tau/2)}{\omega\tau/2}\right]^2\right]\right\}. \quad (2.24)$$

We can obtain a double sum for Γ if we expand the exponential of the sine into a power series and use

$$\int_{-\infty}^{\infty}\frac{d\tau}{(\tau-i\epsilon)^{\beta}}e^{i\lambda\tau}=2\pi\frac{e^{i\pi\beta/2}}{\Gamma(\beta)}\lambda_+^{\beta-1}\ ,$$

(where $\lambda_+=\lambda$ for $\lambda>0$ and $\lambda_+=0$ for $\lambda<0$) to perform the integral over τ. This yields

$$\Gamma=4|E_0|\sum_{s=0}^{\infty}\sum_{n=-s}^{s}(-1)^{n+s}\left[\frac{2(ea)^2|E_0|}{m\omega^2}\right]^s\frac{[n\omega/|E_0|-1-(ea)^2/2m|E_0|]_+^{s+1/2}}{(2s+1)(s-n)!(s+n)!}\ . \tag{2.25}$$

Only positive values of $n\geq N$ contribute to the sum on the rhs. N is the minimum number of photons required for ionization in a weak field.

C. Comparison of the Keldysh-approximation with the exact solution

Ionization from the regularized δ-function well (2.16) has been treated exactly without invoking the Keldysh approximation. We will see that in this case, for most practical purposes, the exact results agree with those obtained from the Keldysh approximation. It was shown[9] that the total ionization rate is determined by the solution of the equation

$$F(\epsilon)=1+i\sum_{s=0}^{\infty}\sum_{n=-s}^{s}(-1)^{n+s}\left[\frac{2(ea)^2|E_0|}{m\omega^2}\right]^s\times\frac{(n\omega/|E_0|+\epsilon)^{s+1/2}}{(2s+1)(s-n)!(s+n)!}=0\ . \tag{2.26}$$

Once a (complex) solution ϵ of this equation has been found, the total ionization rate Γ is determined by

$$\epsilon=-1-\frac{(ea)^2}{2m|E_0|}+\frac{\Delta-\frac{1}{2}i\Gamma}{|E_0|}\ , \tag{2.27}$$

that is

$$\Gamma=-2|E_0|\mathrm{Im}\epsilon\ . \tag{2.28}$$

Equation (2.27) also determines a real field-dependent level shift Δ. This shift does not contain the apparent increase of the ionization potential due to the ponderomotive term $(ea)^2/2m|E_0|$, which is exhibited separately. It is, therefore, small and is normally neglected in the context of above-threshold ionization.

Whenever an ionization *rate* makes any sense, it will be very small, i.e., $\Gamma/2|E_0|$ will be very small compared with unity. Notice that for $s\leq N$ the factor $(n\omega/|E_0|+\epsilon)^{s+1/2}$ on the rhs of Eq. (2.26) is purely imaginary as long as $\mathrm{Im}\epsilon=-\Gamma/2|E_0|$ can be neglected with respect to $[-1-(ea)^2/2m|E_0|+n\omega/|E_0|]$. As just mentioned, this should be an excellent approximation for small enough n. For sufficiently weak fields, certainly for $2(ea)^2|E_0|/(m\omega^2)\ll 1$, an iterative procedure to solve Eq. (2.26) suggests itself whose lowest order consists of dropping Δ and keeping Γ only in the term $s=0$. This yields an explicit equation for Γ which agrees with Eq. (2.25), i.e., this procedure is equivalent with the Keldysh approximation. At first glance it appears that this is only justified for very weak fields satisfying the above condition that $2(ea)^2|E_0|/(m\omega^2)\ll 1$. However, the following argument suggests that the validity can be expected to extend to fields stronger than that. The sum over n in Eq. (2.26) involves very significant cancellations: if the numerator $(\epsilon+n\omega/|E_0|)^{s+1/2}$ is expanded with respect to $n\omega/|E_0|$, then all low-order terms vanish according to

$$\sum_{n=-s}^{s}(-1)^n\frac{n^k}{(s-n)!(s+n)!}=\begin{cases}0, & k<2s\\(-1)^s, & k=2s\end{cases}\ .$$

These cancellations change the effective expansion parameter in Eq. (2.26) from $2(ea)^2|E_0|/(m\omega^2)$ to

$$\left[\frac{2(ea)^2|E_0|}{m\omega^2}\right]\left[\frac{\omega}{|E_0|}\right]^2=\frac{2(ea)^2}{m|E_0|}\ , \tag{2.29}$$

which is in a multiphoton situation typical of ATI smaller than the superficial expansion parameter by about two orders of magnitude. These cancellations explain why the iterative procedure, whose lowest step leads to the Keldysh result (2.25), already gives for all but the strongest fields practically the exact solution of Eq. (2.26). Below, we will quantitatively compare the solution of Eq. (2.26) with Eq. (2.25).

It is also worth mentioning that the differential transition rates (2.20) agree with the exact result [Eq. (17) of Ref. 9] completely up to an overall factor that is the ratio of the exact total ionization rate over the total rate in the Keldysh approximation. Hence, in the case of a δ-function well, the latter exactly predicts the relative strengths of the various channels and their angular distributions.

III. BEHAVIOR OF THE TOTAL IONIZATION RATE

In this section we will investigate the behavior of the total ionization rate as a function of the applied field strength. The discussion will primarily be based on numerical evaluation of the double sum (2.25). A parameter that plays a central role in ATI is the quantity

$$\eta=\frac{(ea)^2}{2m\omega}=(7.53\times10^{-14})\lambda^3 I\ , \tag{3.1}$$

with λ in μm and I in W/cm^2 and a the amplitude of the vector potential as defined in Eq. (2.18). This is the ratio of the height of the ponderomotive barrier $(ea)^2/2m$ over the energy of a laser photon.[16] Hence when $\eta>1$ at least one electron channel is closed due to the ponderomotive barrier. The condition $\eta>1$ also marks the definite onset of nonperturbative behavior of the partial ionization rates into the electron energy channels. We abbreviate

$$w=\frac{\omega}{|E_0|}\ . \tag{3.2}$$

The expansion parameter in the double sum (2.25) for the total rate is

$$\rho^2=\frac{2(ea)^2|E_0|}{m\omega^2}=4\eta/w\ , \tag{3.3}$$

which is in a multiphoton situation larger than η by at least one order of magnitude. However, we argued in Sec. II that the effective expansion parameter may be smaller than this. The quantity

$$\gamma=\frac{\sqrt{2m|E_0|}}{ea}=(\eta w)^{-1/2} \tag{3.4}$$

is called the Keldysh parameter. Its common interpretation is that for $\gamma\gg1$, multiphoton absorption is the predominant mechanism of ionization while for $\gamma\ll1$ it is tunneling.

For a very intense field such that

$$V\ll1,\quad V\gg\omega/|E_0|,\quad \omega/|E_0|\ll1\ , \tag{3.5}$$

where

$$V^2=\frac{(ea\omega)^2}{m|E_0|^3}=2\eta\omega^3=\frac{(eE)^2}{m|E_0|^3}\ , \tag{3.6}$$

(E denotes the electric field amplitude) there is an asymptotic estimate of the total ionization rate[9,12,17]

$$\Gamma\cong\frac{|E_0|V}{2^{3/2}}\exp\left\{-\frac{2^{5/2}}{3V}\left[1-\frac{2}{15}\left[\frac{w}{V}\right]^2\right]\right\}. \tag{3.7}$$

The dependence of this asymptotic formula on w is very weak so that essentially it only depends on V. On the other hand, LOPT, as given by the term of the sum (2.25) with $s=n=N$ and $ea=0$ within the square root, reads

$$\Gamma^{(N)}=4|E_0|\rho^{2N}\frac{(Nw-1)^{N+1/2}}{(2N+1)!}\times\left[1-O\left[\frac{(2N+1)\rho^2w^2}{(Nw-1)}\right]\right], \tag{3.8}$$

where we included on the rhs the order of the next to leading term. We have that $w^{-1}\approx N$ and, under the most favorable conditions, $Nw-1\approx\omega$, so that the order of the leading correction is ρ^2. This would suggest that perturbation theory can only be trusted for $\rho^2\ll1$ and, in fact, breaks down completely when $Nw-1\to0$. LOPT would be out of the question long before the first channel closes because of the ponderomotive barrier.

In order to investigate the transition between the two limits (3.7) and (3.8) we have numerically solved Eq. (2.26) for ϵ and determined Γ from Eq. (2.27). Figure 1 gives the total ionization rate $\Gamma/2|E_0|$ as a function of V on a log-log scale for different values of w. In each case the dot-dashed curve on the right is the asymptotic estimate (3.7). From its derivation it is only a reliable approximation as long as V satisfies the conditions (3.5). The full curve is the solution of Eq. (2.26). The dashed curve represents LOPT, i.e., the first term on the rhs of Eq. (3.8), with $N=3$ for $w=0.5$, $N=5$ for $w=0.22$, and $N=9$ for $w=0.124\,99$. In each case the regions are specified where the asymptotic estimate and LOPT are reasonably trustworthy. One notices that the gap between the regions where one of the two limits applies increases rapidly with decreasing w. For $w=0.124\,99$ the range of LOPT is already outside the figure. In each case, the midpoint between where the rate starts to deviate noticeably from LOPT and where it merges with the asymptotic form (3.7) roughly corresponds to a value of the Keldysh parameter (3.4) of $\sqrt{2}$.

In what follows we will denote by $\mathrm{LOPT}_N(k)$ the leading term on the rhs of Eq. (3.8), but with N, viz., the minimum number of photons required for ionization, replaced by $N+k(k\geq0)$. $\mathrm{LOPT}_N(k)$ corresponds to the

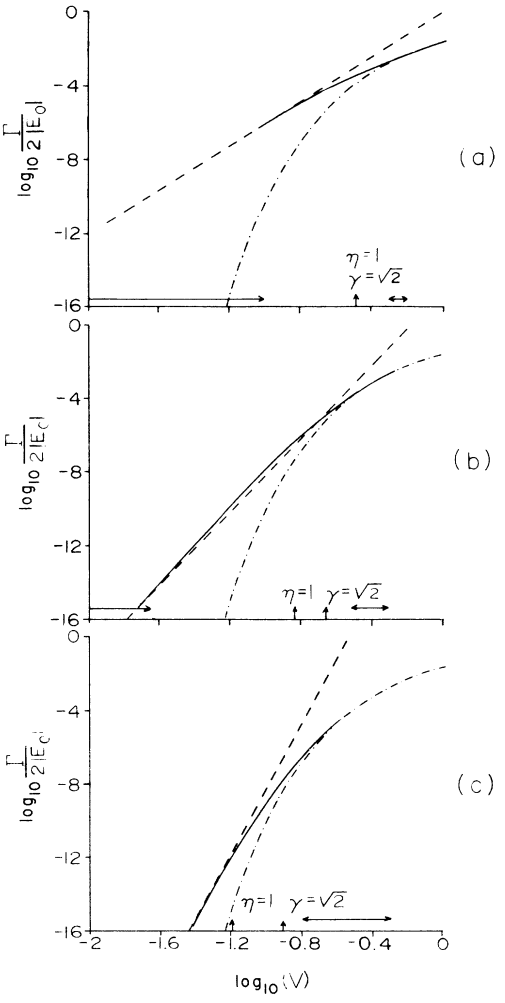

FIG. 1. $\log_{10}(\Gamma/2|E_0|)$ as a function of $\log_{10}V$ for (a) $w=0.5$, (b) $w=0.22$, and (c) $w=0.124\,99$. Solid curve, exact solution from Eq. (2.26); dashed curve, lowest-order perturbation theory; dot-dashed curve, asymptotic estimate (3.7). The vertical arrows on the abscissa specify the values of V where $\eta=1$ and $\gamma=\sqrt{2}$. The arrows parallel to the abcissa indicate the regions of V where LOPT and the asymptotic estimate are reliable approximations.

term in the sum (2.25) with $s=n=N+k$ and $ea=0$ in the square root.

Actually, two of the above cases are such that perturbation theory should not apply at all since $Nw-1$ is either zero or almost zero. What has been labeled as LOPT in Figs. 1(a) and 1(c) was really $\mathrm{LOPT}_N(1)$. Hence it seems that when LOPT appears to become inapplicable, the exact rate prematurely switches to the LOPT result with the next higher value of N. In Fig. 1(b), where $Nw-1$ is about half way between two zeros the exact rate starts with a slope of 5 as expected. It then temporarily adopts a higher slope of approximately 5.5 before it merges with the asymptotic curve.

At $\eta=1$, where the lowest peak of the ATI electron energy spectrum is suppressed, each of the three rates plotted in Figs. 1(a)–1(c) are already quite different from LOPT [be it $\mathrm{LOPT}_N(0)$ for Fig. 1(b) or $\mathrm{LOPT}_N(1)$ for Figs. 1(a)–1(c)]. However, in practice, just by looking at the slope of Γ with respect to I, the deviation from $\mathrm{LOPT}_n(0)$ would be hard to detect. The dependence of Γ on I is still smooth, and the slope is not very different from what one expects from $\mathrm{LOPT}_N(0)$: for $\eta=1$, the slopes are about 2.1, 4.3, and 7.8, respectively, not incompatible with two-, five-, or eight-photon ionization. Also, at no time until the exact rate starts merging with the asymptotic curve is the absolute deviation between LOPT and the exact rate larger than a factor of 5.

It is interesting to notice that the naive expectation that the slope of the total rate at a given intensity might be

$$N_{\min}(I)=N+s(I)\ , \tag{3.9}$$

where $s(I)$ is the number of peaks suppressed at intensity I does not hold true. Rather, the slope increases towards values larger than N already at intensities corresponding to $\eta \ll 1$ where no peak is suppressed yet. At $\eta=1$, the total rate is already bending back from this higher slope toward the asymptotic limit, so that the slope near $\eta=1$ may be close to N again.

Figure 2 gives a more detailed account of the qualitative difference between the exact rate and LOPT. The bold curve is the total ionization rate for fixed $V=0.1$ as a function of w. The various light curves are the $\mathrm{LOPT}_N(0)$ expressions for $2\le N\le 9$. Premature switching to the next highest N is again evident: e.g., the exact result is well approximated by $N=3$ up to about $w=0.52$ at which point $N=2$ quickly takes over. The better LOPT works, the closer should be the agreement between the exact result and one of the LOPT curves. For smaller values of w, the disagreement grows becoming as large as one order of magnitude. Notice, however, the scale of the ordinate, which is very different from Fig. 1, and the fact that $V=0.1$ corresponds to a quite strong field: for $V=0.1$ and $w=0.1$, we have $\eta=5$, i.e., about the lowest five peaks of the electron spectrum have been suppressed.

Figure 3 displays results for higher multiphoton orders comparable to ATI experiments with $\lambda=1064$ μm. A quick glance seems to indicate that LOPT holds almost all the way up $\gamma=\sqrt{2}$ where the curves are about to merge with the asymptotic limit, viz., the dashed curve in the upper right of Fig. 3. A closer look, however, reveals

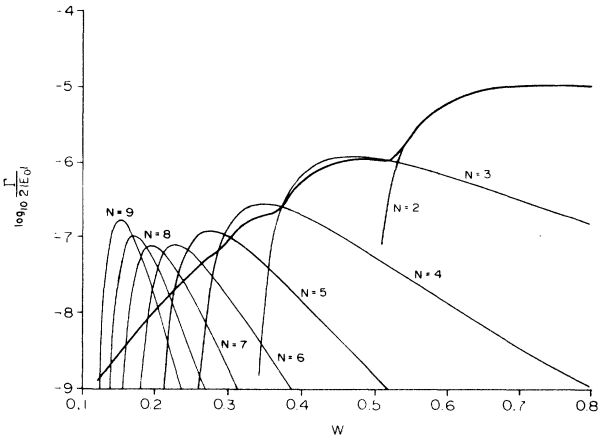

FIG. 2. $\log_{10}(\Gamma/2|E_0|)$ as a function of w for $V=0.1$ (bold curve). The various light curves are the $\mathrm{LOPT}_N(0)$ expressions for $2\le N\le 9$ as labeled.

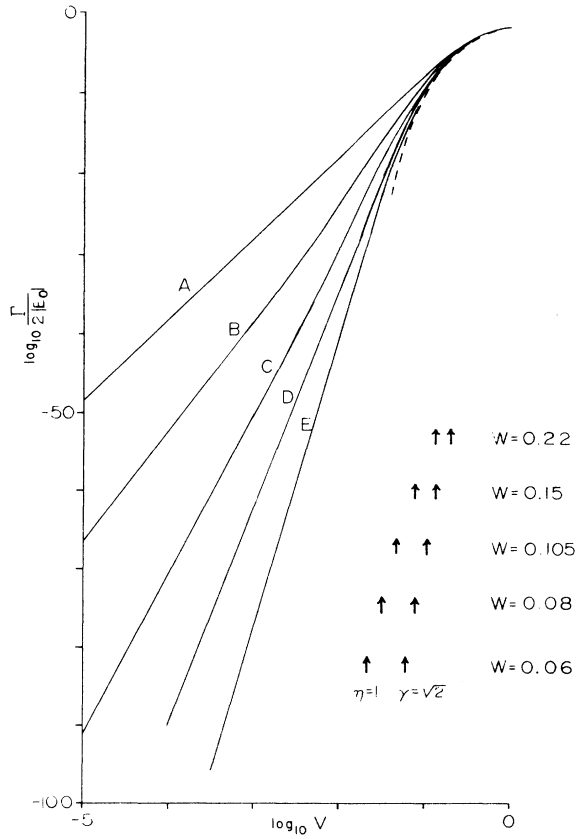

FIG. 3. The logarithm of the total rate as a function of $\log_{10}V$ for various multiphoton orders, curve A $w=0.22(N=5)$, curve B $w=0.15(N=7)$, curve C $w=0.105(N=10)$, curve D $w=0.08(N=13)$, curve E $w=0.06(N=17)$. For curves C, D, and E the actual slopes of the curves are higher than the respective values of N. This is discussed in the text and evident from Table I; it is not visible on the scale of the figure. The dashed curve in the upper right of the figure is the asymptotic estimate (3.7). For each curve, arrows mark the values of V for which $\eta=1$ (at least one channel closed) and $\gamma=\sqrt{2}$ (transition from multiphoton to tunneling regime).

that this is not quite true. The rate for $w=0.105$ follows $\mathrm{LOPT}_{10}(0)$ only up to $V\sim10^{-3}$ (corresponding to $\rho\sim0.13\ll1$); from there on up to $V\lesssim0.1$ it switches to $\mathrm{LOPT}_{10}(1)$. Notice that this already happens for $\eta\ll1$, where one does not expect yet any nonperturbative effects, least of all in the total rate. A superposition of $\mathrm{LOPT}_{10}(0)$ and $\mathrm{LOPT}_{10}(1)$ gives an excellent approximation to the total rate up to $V\sim0.018$ and a fair one (up to within one order of magnitude) up to $V\sim0.07$, cf. Table I(a). The same pattern can be observed for $w=0.08$. Here the exact rate is well approximated by $\mathrm{LOPT}_{13}(1)$ up to $V\sim0.07$; only for $V\lesssim10^{-4}$ does it finally approach $\mathrm{LOPT}_{13}(0)$. Finally, the exact rate for $w=0.06$ is given by $\mathrm{LOPT}_{17}(1)$ from well outside the figure up to $V\sim0.2\times10^{-2}$ where it switches to $\mathrm{LOPT}_{17}(2)$, which is a good approximation up to $V\sim0.03$ [cf. Table I(b)].

It is ironic that, although deviations from $\mathrm{LOPT}_N(0)$ occur at much lower fields than expected, they might not become visible in experiments (better: *gedanken* experiments with an atom well described by a δ-function potential) in the intensity range around and slightly above $\eta=1$, which has been of most interest in ATI experiments. While the slope of the total ionization rate is higher than N at lower intensities, the slope is bending towards the asymptotic limit in just this region. Here, then, the slope is again close to N, viz., the prediction of $\mathrm{LOPT}_N(0)$.

Finally, we should mention that the difference between the solution of Eq. (2.26) and the direct evaluation of the double sum (2.25) is marginal. Numerical results for $w\geq0.125$ have been obtained via the solution of Eq. (2.26) and have been compared with the sum (2.25). Discrepancies approached about 1% near $V=1$ and were much smaller for $V\ll1$. The results for $w\leq0.105$ were derived from the sum (2.25). The alternating character of the sum (2.25) required usage of a multiprecision pack-

TABLE I(a). Logarithm of the total ionization rate $\Gamma/2|E_0|$ as a function of $\log_{10}V$ for $w=0.105$. The parameter η is unity for $\log_{10}V=-1.31$ and $\eta=5$ for $\log_{10}V=-0.97$.

		$\log_{10}(\Gamma/2\|E_0\|)$		
$\log_{10}V$	Eq. (2.25)	$\mathrm{LOPT}_{10}(0)$	$\mathrm{LOPT}_{10}(1)$	$\mathrm{LOPT}_{10}(0)+\mathrm{LOPT}_{10}(1)$
−4	−70.90	−70.91	−73.04	−70.91
−3.25	−55.82	−55.91	−56.54	−55.82
−3.0	−50.67	−50.91	−51.04	−50.66
−2.75	−45.39	−45.91	−45.54	−45.39
−2.5	−40.00	−40.91	−40.04	−40.00
−2.25	−34.54	−35.91	−34.54	−34.52
−2.0	−29.07	−30.91	−29.04	−29.03
−1.75	−23.63	−25.91	−23.54	−23.54
−1.5	−18.29	−20.91	−18.04	−18.04
−1.25	−13.31	−15.91	−12.54	−12.54
−1.0	−9.09	−10.91	−7.04	−7.04

TABLE I(b). Same as Table I(a) for $w=0.06$. The parameter η equals 1 at $\log_{10}V=-1.68$ and $\eta=5$ at $\log_{10}V=-1.33$.

		$\log_{10}(\Gamma/2\|E_0\|)$			
$\log_{10}V$	Eq. (2.25)	$\mathrm{LOPT}_{17}(0)$	$\mathrm{LOPT}_{17}(1)$	$\mathrm{LOPT}_{17}(2)$	$\mathrm{LOPT}_{17}(0)+\mathrm{LOPT}_{17}(1)$ $\mathrm{LOPT}_{17}(2)$
−5	−149.73	−151.24	−149.74	−154.08	−149.73
−4.0	−113.74	−117.24	−113.74	−116.08	−113.74
−3.5	−95.72	−100.24	−95.74	−97.08	−95.72
−3.25	−86.68	−91.74	−86.74	−87.58	−86.68
−3.0	−77.56	−83.24	−77.74	−78.08	−77.58
−2.75	−68.37	−74.76	−68.74	−68.58	−68.35
−2.5	−59.02	−66.24	−59.74	−59.08	−59.00
−2.25	−49.58	−57.75	−50.74	−49.58	−49.55
−2.0	−40.13	−49.24	−41.74	−40.08	−40.07
−1.75	−30.87	−40.74	−32.74	−30.58	−30.58
−1.5	−22.27	−32.24	−23.74	−21.08	−21.08
−1.25	−16.32	−23.74	−14.74	−11.58	
−1.0	−9.62	−15.24	−5.74	−2.08	

age. Up to 75 valid digits had to be kept to obtain the smooth connection between LOPT and the asymptotic limit.

IV. CONCLUSIONS

An interesting observation made in this paper is that the Keldysh approximation for a short-range potential with just one bound state is virtually exact. This was noticed by direct comparison of Berson's exact solution[9] with the corresponding Keldysh approximation. This fact may be not too surprising. For the two approximations made by Keldysh, viz., ignoring all bound states of the atom besides the initial ground state and replacing the continuum states of the binding potential by plane waves, are not much of an approximation for a δ-function potential with only one bound state. What *is* neglected by the Keldysh approximation even in this context is the possibility of repeated virtual transitions between the ground state and continuum states (viz., Rabi oscillations between the ground state and the continuum leading to the very small real level shift Δ) and the exact form of the continuum wave functions at the origin. Both approximations are much more questionable for a long-range potential. In fact, simulations of a one-dimensional model with a long-range potential have exhibited[18] poor agreement between the exact calculated transition probability and the Keldysh approximation. Moreover, the KFR model (evaluated with hydrogenlike wave functions) does not fit the experimental data very well over a range of intensities.[19] For a one-dimensional δ-function potential, however, and a constant electric field, it has been shown that the Keldysh approximation gives good results.[20]

Surprisingly, in a multiphoton situation where ten and more photons are required for ionization, lowest-order perturbation theory [denoted above by $\mathrm{LOPT}_N(0)$], strictly speaking, only holds up to very low intensities, much lower than those employed in ATI experiments. For any intensity of experimental interest that leads to a measurable ionization rate, the slope of the total ionization rate versus intensity comes out to be $N+1$ or even $N+2$ [denoted above by $\mathrm{LOPT}_N(1)$ and $\mathrm{LOPT}_N(2)$] in place of N, which is predicted by $\mathrm{LOPT}_N(0)$. This has nothing to do with the apparent increase of the binding potential by the ponderomotive potential. Rather it is related to the fact that the phase space for low-energy electrons is very small. The increase of the slope from N to $N+1$ and $N+2$ already occurs at intensities so low that the ponderomotive potential plays no role yet. On a log-log scale as used in Fig. 3, this change in the slope is hardly visible. The perturbation theory curves for different values of $\omega/|E_0|$ appear to make a perfect tangent bundle to the asymptotic curve which is independent of $\omega/|E_0|$. The transition from one to the other occurs for a value of the Keldysh parameter of about $\sqrt{2}$.

Since the curves have to bend from the large slope of perturbation theory to the much smaller slope of the asymptotic curve, there is a region in between where the slope is again near N, the value of $\mathrm{LOPT}_N(0)$. This region is around $\eta=1$ where most experiments have been performed all of which yielded slopes near N. In spite of that, one would rather conclude that experimental evidence speaks against the applicability of a short-range model to ATI phenomena. For in no case has the slope of $N+1$ or $N+2$ predicted at low intensities by this model been observed. Moreover, experiments also seem to indicate that the I^N dependence of the total ionization rate persists up to higher intensities than found here.[2,3]

ACKNOWLEDGMENTS

We benefitted from discussions with M. Kleber, and we are indebted to S. Long for a careful reading of the manuscript.

APPENDIX

An integration by parts with respect to time led from Eq. (2.8) to Eq. (2.10). The boundary terms at $t=\pm\infty$ safely vanish for a field pulse of finite duration. In Sec. II C, however, we evaluated Eq. (2.10) for the monochromatic field (2.18), which is of infinite extent. It is not quite clear in this case whether the equality of the expressions (2.8) and (2.10) still holds. In this appendix we will, therefore, reevaluate the matrix element $M_{\mathrm{p}}^{(K)}$ using Eq. (2.8).

From Eqs. (2.8) and (2.9), we have

$$M_{\mathrm{p}}^{(K)}=\frac{1}{(2\pi)^{3/2}}\int d^3r\,dt\,\exp\left[\frac{i}{2m}\int^t d\tau\,\pi^2(\tau)\right]\times\left[-\frac{\partial}{\partial t}e^{-i\pi(t)\cdot(\mathbf{r})}\right]\psi_0^{(0)}(\mathbf{r},t)\ . \tag{A1}$$

Above, in the calculation in Sec. II C, the gauge phase $\exp[ie\,\mathbf{A}(t)\cdot\mathbf{r}]$ cancelled due to the presence of the δ-function potential. Its presence here makes the evaluation much more cumbersome. For the field (2.18) we expand both exponentials in terms of Bessel functions and perform the integration over time with the result

$$M_{\mathrm{p}}^{(K)}=-\frac{i\omega\sqrt{\kappa}}{2\pi}\int\rho\,d\rho\,dz\,d\phi\frac{\exp[-\kappa(\rho^2+z^2)^{1/2}]}{(\rho^2+z^2)^{1/2}}\exp[-i(p_z z+\rho p_T\cos\phi)]\times\sum_{n,s}\delta\left[\frac{\mathbf{p}^2+(ea)^2}{2m}+|E_0|-n\omega\right]\times(s-n)J_s\left[\frac{eap_T}{m\omega}\right]J_{s-n}(ea\rho)\exp(-in\delta)\exp[i(n-s)(\phi-\pi)]\ .$$

The integrations over z and ϕ are readily done yielding

$$M_{\mathbf{p}}^{(K)}=-i2\omega\sqrt{\kappa}\sum_{n,s}(s-n)\delta\left[\frac{\mathbf{p}^2+(ea)^2}{2m}+|E_0|-n\omega\right]e^{-in\delta}J_s\left[\frac{eap_T}{m\omega}\right]\int_0^\infty\rho\,d\rho\,K_0[\rho(p_z^2+\kappa^2)^{1/2}]J_{s-n}(ea\rho)J_{s-n}(p_T\rho)\ .$$

The remaining integration with respect to ρ leads to

$$M_{\mathbf{p}}^{(K)}=-\frac{i}{m}\sqrt{\kappa}\sum_{n,s}(s-n)\delta\left[\frac{\mathbf{p}^2+(ea)^2}{2m}+|E_0|-n\omega\right]e^{-in\delta}J_s(z)\frac{1}{(n^2-z^2)^{1/2}}\left[\frac{n-(n^2-z^2)^{1/2}}{z}\right]^{|n-s|}$$

where $z=eap_T/m\omega$. This agrees with Eq. (2.19) provided that

$$(n^2-z^2)^{1/2}J_n(z)=-\sum_{s=-\infty}^{\infty}(s-n)J_s(z)\left[\frac{n-(n^2-z^2)^{1/2}}{z}\right]^{|s-n|}$$

holds. This formula is easily proven by using an integral representation for $J_s(z)$ on the right-hand side.

[1]P. Agostini, F. Fabre, G. Mainfray, G. Petite, and N. K. Rahman, Phys. Rev. Lett. **42**, 1127 (1979); P. Kruit, J. Kimman, H. G. Muller, and M. J. van der Wiel, Phys. Rev. A **28**, 248 (1983).

[2]L. A. Lompré, G. Mainfray, and C. Manus, J. Phys. B **13**, 85 (1980).

[3]H. G. Muller, H. B. van Linden van den Heuvell, P. Agostini, G. Petite, A. Antonetti, M. Franco, and A. Migus, Phys. Rev. Lett. **60**, 565 (1988).

[4]H. G. Muller and A. Tip, Phys. Rev. A **30**, 3039 (1984); J. Zakrzewski and K. Zyczkowski, *ibid.* **36**, 4311 (1987); A. Giusti-Suzor and P. Zoller, *ibid.* **36**, 5178 (1987).

[5]H. R. Reiss, Phys. Rev. A **22**, 1786 (1980).

[6]E. Fermi, Ric. Sci. **7**, 13 (1936).

[7]G. Breit, Phys. Rev. **71**, 215 (1947); J. M. Blatt and V. F. Weisskopf, *Theoretical Nuclear Physics* (Wiley, New York, 1952), pp. 74–75.

[8]K. Huang and C. N. Yang, Phys. Rev. **105**, 767 (1957); T. D. Lee, K. Huang, and C. N. Yang, *ibid.* **106**, 1134 (1957); T. T. Wu, *ibid.* **115**, 1390 (1959).

[9]I. J. Berson, J. Phys. B **8**, 3078 (1975).

[10]G. P. Arrighini, C. Guidotti, and N. Durante, Nuovo Cimento **7D**, 559 (1986).

[11]G. P. Arrighini, G. Guidotti, and N. Durante, Phys. Rev. A **35**, 1528 (1987).

[12]N. B. Delone and V. P. Krainov, in *Atoms in Strong Light Fields,* Vol. 28 of *Springer Series in Chemical Physics,* edited by V. I. Goldanskii, R. Gomer, F. P. Schäfer, and J. P. Toennies (Springer, Berlin, 1985).

[13]L. V. Keldysh, Zh. Eksp. Teor. Fiz. **47**, 1945 (1964) [Sov. Phys.—JETP **20**, 1307 (1965)].

[14]F. H. M. Faisal, J. Phys. B **6**, L312 (1973).

[15]H. R. Reiss, J. Phys. B **20**, L79 (1987); J. Opt. Soc. Am. B **4**, 726 (1987).

[16]For a discussion of the role of the ponderomotive potential in ATI, see, for example, P. H. Bucksbaum, R. R. Freeman, M. Bashkansky, and T. J. McIlrath, J. Opt. Soc. Am. B **4**, 760 (1987).

[17]N. L. Manakov and P. L. Rapoport, Zh. Eksp. Teor. Fiz. **69**, 842 (1975).

[18]L. A. Collins and A. L. Merts, Phys. Rev. A **37**, 2415 (1988); J. N. Bardsley, A. Szöke, and M. J. Comella, J. Phys. B **21**, 3899 (1988); J. Javanainen and J. H. Eberly, Phys. Rev. A **39**, 458 (1989).

[19]G. Petite, P. Agostini, and H. G. Muller, J. Phys. B **21**, 4097 (1988).

[20]W. Elberfeld and M. Kleber, Z. Phys. B **73**, 23 (1988).